Pilot Symbol Aided Channel Estimation for OCDM Transmissions

Muhammad Shahmeer Omar and Xiaoli Ma

***Abstract*—Pilot-aided channel estimation allows the receiver to acquire channel state information (CSI) for each multicarrier block by multiplexing data and pilot symbols in the same block, as long as they can be decoupled. This work proposes several frequency-domain pilot multiplexing techniques to enable independent channel estimation and detection at the receiver for orthogonal chirp division multiplexing (OCDM) transmissions in frequency-selective channels. Analysis shows that each of the proposed schemes is able to achieve the mean squared error (MSE) lower bound for channel estimation and has greater spectral efficiency than the existing schemes for OCDM and chirp spread orthogonal frequency division multiplexing (OFDM).**

***Index Terms*—Orthogonal chirp division multiplexing, channel estimation, chirp spread OFDM**

I. Introduction

Orthogonal chirp division multiplexing (OCDM) modulates data using orthogonal chirps, thus spreading them over the entire signal bandwidth, which enables better bit error rate (BER) performance in frequency selective channels and makes it more robust to both time-limited and frequency-limited interference than orthogonal frequency division multiplexing (OFDM) [1], [2]. It also shows advantages in the class of unitary modulations for time and frequency-selective channels when modulation alphabet and block size are finite [3].

Wireless channels can be estimated by transmitting a sequence of symbols that are known at the receiver. These known symbols can be transmitted as dedicated blocks, called preamble training (e.g., [4], [5]), or they can be multiplexed in the same block as the data, heretofore referred to as pilots. A preamble-based method for OCDM in frequency-selective channels was proposed in [4] using an unmodulated chirp as preamble and windowing to improve estimate quality. Similarly, a unique-word based approach was adopted in [5] for OCDM in doubly selective channels.

A vital condition of preamble training is that the time difference between successive preambles in a frame needs to be smaller than the channel coherence time. Failure to meet this criterion may result in performance loss. Pilot-based methods, such as those used in OFDM (see e.g. [6], [7], [8]) mitigate the requirement, and simultaneously enhance spectral efficiency.

In this letter, we design pilot-based channel estimation methods for OCDM. More specifically, we outline various techniques to multiplex pilot and data symbols at the transmitter and decouple channel estimation with symbol detection at the receiver. The proposed transmitting structure also subsumes our previous work on spectrum control and multi-user transmissions [9], [10] as special cases. We show that each of these OCDM channel estimators achieves the lower bound of the mean squared error (MSE) while having higher spectral efficiency than existing ones for OCDM and chirp spread (cs-)OFDM in [4], [8], respectively.

M. S. Omar and X. Ma are with the School of Electrical and Computer Engineering, Georgia Institute of Technology, Atlanta, GA 30332, USA (emails: momar6@gatech.edu; xiaoli@gatech.edu)

This work is, in part, supported by an Industry/University Cooperative Research center of National Science Foundation Center on Fiber Wireless Integration and Networking (FiWIN) for heterogeneous mobile data communications under contract number 1539976.

II. System Model

A. OCDM transmissions

In OCDM, a length$-N$ block of complex symbols $\mathbf{x}(i) = [x(iN),\ x(iN+1),\ ...,\ x(iN+N-1)]^T$, where $(.)^T$ denotes the matrix transpose, is modulated using the inverse DFnT (IDFnT) to result in the block given by $\mathbf{\Phi}_N^{\mathcal{H}}\mathbf{x}(i)$, where the DFnT matrix is defined as

$$\Phi(m,n) = \frac{1}{\sqrt{N}} e^{-j\frac{\pi}{4}} \times \begin{cases} e^{j\frac{\pi}{N}(m-n)^2} & N \equiv 0 \text{ (mod 2)} \\ e^{j\frac{\pi}{N}(m+\frac{1}{2}-n)^2} & N \equiv 1 \text{ (mod 2),} \end{cases} \quad (1)$$

and $(.)^{\mathcal{H}}$ denotes the conjugate transpose. After appending cyclic prefix (CP), the block passes through a parallel-to-serial (P/S) converter, pulse-shaping filter, digital-to-analog converter (DAC) and radio front-end pre-processors before being transmitted. Assume that the CP duration is greater than the maximum channel delay spread, i.e., there is no inter-block interference (IBI). Thus, after removing the CP, the i^{th} received block is given by

$$\tilde{\mathbf{y}}(i) = \tilde{\mathbf{H}}_i \mathbf{\Phi}_N^{\mathcal{H}} \mathbf{x}(i) + \tilde{\mathbf{w}}(i), \quad (2)$$

where $\tilde{\mathbf{H}}_i$ is an $N \times N$ column-wise circulant matrix with the first column given by $[h_i(0),\ h_i(1),\ ...,\ h_i(L),\ 0,\ ...,\ 0]^T$, with $h_i(n)$, $\forall n \in [0,\ L]$ being the n^{th} channel tap for the i^{th} block, and $\tilde{\mathbf{w}}(i)$ represents the additive noise. Since there is no IBI, each block can be processed independently. Thus, the block index i is dropped for simplicity.

Due to its lower complexity, we consider only frequency domain equalization in this work. The frequency-domain block, after phase correction, is given by

$$\mathbf{\Gamma}_N \mathbf{F}_N \tilde{\mathbf{y}} = \mathbf{D}_h \mathbf{F}_N \mathbf{x} + \mathbf{\Gamma}_N \mathbf{F}_N \tilde{\mathbf{w}}, \quad (3)$$

where $\mathbf{D}_h = \text{diag}([H(0),\ ...,\ H(N-1)])$ is an $N \times N$ diagonal matrix containing the channel frequency response (CFR) on its main diagonal, given by $H(k)$, $\forall k \in [0, N-1]$, $\mathbf{\Gamma}_N = \mathbf{F}_N \mathbf{\Phi}_N \mathbf{F}_N^{\mathcal{H}}$ is a diagonal matrix containing the eigenvalues of $\mathbf{\Phi}$, which have been defined in [1, Eq. (30)], and $\mathbf{F}_N$ is an $N \times N$ normalized DFT matrix. The resulting symbols are equalized and converted back to the time domain prior to detection.

This article has been accepted for publication in a future issue of this journal, but has not been fully edited. Content may change prior to final publication. Citation information: DOI 10.1109/LCOMM.2021.3124627, IEEE Communications Letters

B. Affine data and pilot transmission

Consider general block transmissions with CP in a wireless multipath channel, where each length$-N$ block contains N_p pilots and N_d data symbols such that $N = N_p + N_d$. Define $\mathbf{u} = [u(0),\ u(1),\ ...,\ u(N_d-1)]^T$ as the data sub-block and $\mathbf{b} = [b(0),\ b(1),\ ...,\ b(N_p-1)]^T$ as the pilot sub-block. In order to multiplex pilot and data symbols in the same block, we define the transmitted block as

$$\mathbf{x} = \mathbf{A}_d\mathbf{u} + \mathbf{A}_p\mathbf{b}, \tag{4}$$

where $\mathbf{A}_d$ and $\mathbf{A}_p$ are general transmitter matrices with dimension $N \times N_d$ and $N \times N_p$ for the data and pilot sub-blocks, respectively. These matrices subsume the modulation and multiplexing operations for each sub-block. After removing the CP, the received block is given by

$$\tilde{\mathbf{y}} = \tilde{\mathbf{H}}\mathbf{x} + \tilde{\mathbf{w}} = \tilde{\mathbf{H}}\mathbf{A}_d\mathbf{u} + \tilde{\mathbf{H}}\mathbf{A}_p\mathbf{b} + \tilde{\mathbf{w}}. \tag{5}$$

Noting that $\tilde{\mathbf{H}} = \mathbf{F}_N^{\mathcal{H}}\mathbf{D}_h\mathbf{F}_N$, it is easy to see that multiplexing pilots in the frequency domain decouples channel estimation and data detection at the receiver. Let us define $\tilde{\mathbf{A}}_d = \mathbf{F}_N\mathbf{A}_d$ and $\tilde{\mathbf{A}}_p = \mathbf{F}_N\mathbf{A}_p$ as the frequency-domain transmitter matrices for the data and pilot sub-blocks, respectively. Hence, Eq. (5) becomes

$$\tilde{\mathbf{y}} = \mathbf{F}_N^{\mathcal{H}}\mathbf{D}_h\tilde{\mathbf{A}}_d\mathbf{u} + \mathbf{F}_N^{\mathcal{H}}\mathbf{D}_h\tilde{\mathbf{A}}_p\mathbf{b} + \tilde{\mathbf{w}}. \tag{6}$$

Performing the DFT, we get

$$\mathbf{F}_N\tilde{\mathbf{y}} = \mathbf{D}_h\tilde{\mathbf{A}}_d\mathbf{u} + \mathbf{D}_h\tilde{\mathbf{A}}_p\mathbf{b} + \mathbf{F}_N\tilde{\mathbf{w}}. \tag{7}$$

Let us define matrices $\tilde{\mathbf{A}}_d^{\dagger}$ and $\tilde{\mathbf{A}}_p^{\dagger}$ such that the received pilot and data sub-blocks are given by $\tilde{\mathbf{A}}_p^{\dagger}\mathbf{F}_N\tilde{\mathbf{y}}$ and $\tilde{\mathbf{A}}_d^{\dagger}\mathbf{F}_N\tilde{\mathbf{y}}$, respectively. Thus, it is easy to see that decoupled channel estimation and detection is only possible when $\tilde{\mathbf{A}}_d^{\dagger}\mathbf{D}_h\tilde{\mathbf{A}}_p = \tilde{\mathbf{A}}_p^{\dagger}\mathbf{D}_h\tilde{\mathbf{A}}_d = \mathbf{0}$.

Thus far, we have introduced a general multiplexing method that is applicable to any form of precoded OFDM as seen in Eq. (6). However, the definitions of the transceiver matrices depend on the type of precoding being used. We will define the matrices for OCDM in subsequent sections.

III. Pilot Multiplexing

Let us introduce some definitions that will be used in the remainder of this section. Let $\mathcal{I} = \{n:\ 0 \le n < N \text{ and } n_i > n_t\ \forall i > t\}$ be the ordered set of indices of a vector $\mathbf{y}$. Let $\mathcal{I}_l = \{n_k:\ \forall k \in [0,\ |\mathcal{I}_l|-1] \text{ and } n_i > n_t\ \forall i > t\} \subseteq \mathcal{I}$, where $|\mathcal{I}_l|$ is the set cardinality, such that $\cup_l \mathcal{I}_l = \mathcal{I}$ and $\mathcal{I}_l \cap \mathcal{I}_k = \emptyset,\ \forall k \ne l$. Now, we can define the $|\mathcal{A}| \times N$ multiplexing matrix $\mathbf{T}_{\mathcal{A}}$ for a general ordered set $\mathcal{A}$ as $T_{\mathcal{A}}(a,b) = 1$ if $b = \mathcal{A}(a)$ and 0, otherwise. We use the shorthand $\mathcal{A}(a) = n_a$ to denote the a^{th} element of the set $\mathcal{A}$ for convenience. Thus, for L sub-blocks, the multiplexed vector is given by $\mathbf{y} = \sum_{l=0}^{L-1}\mathbf{T}_{\mathcal{I}_l}^T\mathbf{x}_l$.

A. Multicarrier (mc-)OCDM

Inspired by Eq. (6), one way to decouple the sub-blocks is to move the OCDM modulator into the frequency domain and modulate a subset of the sub-carriers. Defining $\mathcal{I}_p$ as the pilot subcarrier indices and $\mathcal{I}_d = \mathcal{I} \setminus \mathcal{I}_p$ as the data subcarrier indices, the resulting received block is given by

$$\tilde{\mathbf{y}} = \tilde{\mathbf{H}}\mathbf{F}_N^{\mathcal{H}}\mathbf{T}_{\mathcal{I}_d}^T\mathbf{\Phi}_{N_d}^{\mathcal{H}}\mathbf{u} + \tilde{\mathbf{H}}\mathbf{F}_N^{\mathcal{H}}\mathbf{T}_{\mathcal{I}_p}^T\mathbf{b} + \tilde{\mathbf{w}}. \tag{8}$$

We call this waveform multicarrier (mc-)OCDM. Comparing with Eq. (6), we see that $\tilde{\mathbf{A}}_d = \mathbf{T}_{\mathcal{I}_d}^T\mathbf{\Phi}_{N_d}^{\mathcal{H}}$ and $\tilde{\mathbf{A}}_p = \mathbf{T}_{\mathcal{I}_p}^T$. The receiver matrices can subsequently be defined as $\tilde{\mathbf{A}}_d^{\dagger} = \mathbf{\Phi}_{N_d}^{\mathcal{H}}\mathbf{G}\mathbf{T}_{\mathcal{I}_d}$, where $\mathbf{G}$ denotes the equalizer, and $\tilde{\mathbf{A}}_p^{\dagger} = \mathbf{T}_{\mathcal{I}_p}$. Since $\mathcal{I}_p \cap \mathcal{I}_d = \emptyset$ by definition, it follows that $\tilde{\mathbf{A}}_d^{\dagger}\mathbf{D}_h\tilde{\mathbf{A}}_p = \tilde{\mathbf{A}}_p^{\dagger}\mathbf{D}_h\tilde{\mathbf{A}}_d = \mathbf{0}$ thus, satisfying the decoupling condition.

Mc-OCDM spreads the data symbols over a smaller set of subcarriers, using the remaining for pilots. This can be extended by dividing a length$-N$ block into M blocks of length K such that $N = MK$, and spreading over each sub-block. Along this line, we define $\mathcal{I}_m = \{m + Mn:\ n \in [0,\ K-1] \text{ and } n_i > n_t\ \forall i > t\}$ as the subcarrier indices for the m^{th} group, where $0 \le m \le M-1$. Without loss of generality (WLOG), we set $\mathcal{I}_p = \mathcal{I}_0$. The resultant waveform, called grouped (g-)OCDM, is given by

$$\tilde{\mathbf{y}} = \tilde{\mathbf{H}}\sum_{m=1}^{M-1}\mathbf{F}_N^{\mathcal{H}}\mathbf{T}_{\mathcal{I}_m}^T\mathbf{\Phi}_K^{\mathcal{H}}\mathbf{u}_m + \tilde{\mathbf{H}}\mathbf{F}_N^{\mathcal{H}}\mathbf{T}_{\mathcal{I}_p}^T\mathbf{\Phi}_K^{\mathcal{H}}\mathbf{b} + \tilde{\mathbf{w}}. \tag{9}$$

Using the definition $\tilde{\mathbf{A}}_d^{(m)} = \mathbf{T}_{\mathcal{I}_m}^T\mathbf{\Phi}_K^{\mathcal{H}}$, we define $\tilde{\mathbf{A}}_d = [\tilde{\mathbf{A}}_d^{(1)},\ \tilde{\mathbf{A}}_d^{(2)},\ ...,\ \tilde{\mathbf{A}}_d^{(M-1)}]$ and $\tilde{\mathbf{A}}_p = \mathbf{T}_{\mathcal{I}_p}^T\mathbf{\Phi}_K^{\mathcal{H}}$. Hence, the receiver matrix for the m^{th} data sub-block is given by $\tilde{\mathbf{A}}_d^{(m)\dagger} = \mathbf{\Phi}_K\mathbf{G}_m\mathbf{T}_{\mathcal{I}_m}$, where $\mathbf{G}_m$ is the equalizer matrix for the m^{th} sub-block, and the one for the pilot sub-block is given by $\tilde{\mathbf{A}}_p^{\dagger} = \mathbf{\Phi}_K\mathbf{T}_{\mathcal{I}_p}$. Noting that $\mathcal{I}_p \cap \mathcal{I}_m = \emptyset,\ \forall m \in [1,\ M-1]$, it follows that the decoupling condition is satisfied.

B. Frequency shift precoded (fsp-)OCDM

The fsp-OCDM design was proposed in [9] for multi-user OCDM transmissions and is subsumed by the affine transmission model in Eq. (5) by setting $\mathbf{A}_d^{(m)} = \mathbf{\Phi}_N^{\mathcal{H}}\mathbf{\Delta}_m\mathbf{P}$, where $\mathbf{\Delta}_m$ and $\mathbf{P}$ are defined in [9, Eq. (9)]. Based on the properties of the precoder and IDFnT matrices, and the definition of $\mathcal{I}_m$ from the previous subsection, the received block is given by

$$\tilde{\mathbf{y}} = \mathbf{F}_N^{\mathcal{H}}\mathbf{D}_h\mathbf{\Gamma}_N^{\mathcal{H}}\left(\sum_{m=1}^{M-1}\mathbf{T}_{\mathcal{I}_m}^T\mathbf{F}_K\mathbf{u}_m + \mathbf{T}_{\mathcal{I}_0}^T\mathbf{F}_K\mathbf{b}\right) + \tilde{\mathbf{w}}, \tag{10}$$

where we have dedicated one sub-block to pilots and the rest to data. Thus, the transmitter matrices are given for the m^{th} data sub-block and pilot sub-block are given by $\tilde{\mathbf{A}}_d^{(m)} = \mathbf{\Gamma}_N^{\mathcal{H}}\mathbf{T}_{\mathcal{I}_m}^T\mathbf{F}_K$ and $\tilde{\mathbf{A}}_p = \mathbf{\Gamma}_N^{\mathcal{H}}\mathbf{T}_{\mathcal{I}_0}^T\mathbf{F}_K$, respectively. The corresponding receiver matrices are given by $\tilde{\mathbf{A}}_d^{(m)\dagger} = \mathbf{F}_K^{\mathcal{H}}\mathbf{G}_m\mathbf{T}_{\mathcal{I}_m}\mathbf{\Gamma}_N$, and $\tilde{\mathbf{A}}_p^{\dagger} = \mathbf{F}_K^{\mathcal{H}}\mathbf{T}_{\mathcal{I}_0}\mathbf{\Gamma}_N$. Comparing Eq. (10) and Eq. (9), we can see that the two are very similar, with the only difference being the spreading matrices. Therefore, due to reasoning similar to g-OCDM, fsp-OCDM satisfies the decoupling condition.

C. Constrained (c-)OCDM

C-OCDM [10] was designed for spectrum control. In order to enable pilot multiplexing, we partition the available bandwidth into M sub-bands with K subcarriers, where each sub-band corresponds to one sub-block. In each sub-band, we utilize only $J = K-1$ subcarriers for spreading data, leaving M subcarriers for pilots. Thus, in this case, $N_p = M$ and the pilot subcarrier indices are given by $\mathcal{I}_p = \{nK:\ \forall n \in [0,\ M-1] \text{ and } n_i < n_t,\ \forall i < t\}$. The data subcarriers in the m^{th} sub-band are given by $\mathcal{I}_m = \{mK + 1 + n:\ \forall n \in [0,\ J-1] \text{ and } n_i < n_t,\ \forall i < t\}$. The resultant received block is then given by (c.f. [10, Eq. (7)])

$$\tilde{\mathbf{y}} = \mathbf{F}_N^{\mathcal{H}}\mathbf{D}_h\left(\sum_{m=0}^{M-1}\mathbf{T}_{\mathcal{I}_m}^T\mathbf{\Gamma}_J^{\mathcal{H}}\mathbf{F}_J\mathbf{u}_m + \mathbf{T}_{\mathcal{I}_p}^T\mathbf{b}\right) + \tilde{\mathbf{w}}. \tag{11}$$

This article has been accepted for publication in a future issue of this journal, but has not been fully edited. Content may change prior to final publication. Citation information: DOI 10.1109/LCOMM.2021.3124627, IEEE Communications Letters

Eq. (11) and the definition of $\mathcal{I}_m$ shows that c-OCDM sub-blocks are multiplexed in the frequency domain with spreading taking place over a localized group of subcarriers. The transmitter matrices for the m^{th} data sub-block and pilot sub-block are given by $\tilde{\mathbf{A}}_d^{(m)} = \mathbf{T}_{\mathcal{I}_m}^T \mathbf{\Gamma}_J^{\mathcal{H}} \mathbf{F}_J$ and $\tilde{\mathbf{A}}_p = \mathbf{T}_{\mathcal{I}_p}^T$. The corresponding receiver matrices are given by $\tilde{\mathbf{A}}_d^{(m)\dagger} = \mathbf{F}_J^{\mathcal{H}} \mathbf{G}_m \mathbf{\Gamma}_J \mathbf{T}_{\mathcal{I}_m}$, and $\tilde{\mathbf{A}}_p^{\dagger} = \mathbf{T}_{\mathcal{I}_p}$. Since $\mathcal{I}_m \cap \mathcal{I}_p = \emptyset,\ \forall m \in [0,\ M-1]$, the decoupling condition is satisfied.

Instead of spreading over contiguous subcarriers, interleaved (i)c-OCDM is designed to spread data over an interleaved subset of subcarriers for each sub-block. In this case, the m^{th} sub-block index set is defined as $\mathcal{I}_m = \{m + Mn :\ n \in [0,\ K-1] \text{ and } n_i > n_t\ \forall i > t\}$ and $\mathcal{I}_p = \mathcal{I}_0$. Thus, the received block is given by

$$\tilde{\mathbf{y}} = \mathbf{F}_N^{\mathcal{H}} \mathbf{D}_h \left(\sum_{m=1}^{M-1} \mathbf{T}_{\mathcal{I}_m}^T \mathbf{\Gamma}_K^{\mathcal{H}} \mathbf{F}_K \mathbf{u}_m + \mathbf{T}_{\mathcal{I}_p}^T \mathbf{\Gamma}_K^{\mathcal{H}} \mathbf{F}_K \mathbf{b} \right) + \tilde{\mathbf{w}}. \quad (12)$$

It can be seen that the block given in Eq. (12) is very similar to the one in Eq. (11), with the difference primarily being in the subcarrier indices used to multiplex the data sub-blocks. Hence, the data sub-block transmitter and receiver matrices are the same as in c-OCDM. The pilot matrices are given by $\tilde{\mathbf{A}}_p = \mathbf{T}_{\mathcal{I}_p}^T \mathbf{\Gamma}_K^{\mathcal{H}} \mathbf{F}_K$ and $\tilde{\mathbf{A}}_p^{\dagger} = \mathbf{F}_K^{\mathcal{H}} \mathbf{\Gamma}_K \mathbf{T}_{\mathcal{I}_p}$.

IV. Channel Estimators

The transmitter matrices for each of the schemes in the previous section can be generalized as $\tilde{\mathbf{A}}_p = \mathbf{T}_{\mathcal{I}_p}^T \mathbf{B}$, where $\mathbf{B}$ depends on the scheme being used and will already be known by the receiver. Thus, isolating the pilots results in

$$\begin{aligned} \hat{\mathbf{b}} = \mathbf{T}_{\mathcal{I}_p} \mathbf{F}_N \tilde{\mathbf{y}} &= \mathbf{T}_{\mathcal{I}_p} \mathbf{F}_N \mathbf{D}_h \mathbf{T}_{\mathcal{I}_p}^T \mathbf{B}\mathbf{b} + \mathbf{T}_{\mathcal{I}_p} \mathbf{F}_N \tilde{\mathbf{w}}, \\ &= \underbrace{\mathbf{D}_b \mathbf{T}_{\mathcal{I}_p} \mathbf{V}}_{\mathbf{W}} \mathbf{h} + \mathbf{T}_{\mathcal{I}_p} \mathbf{F}_N \tilde{\mathbf{w}}, \end{aligned} \quad (13)$$

where $\mathbf{V}$ is an $N \times (L+1)$ matrix containing the leading $L+1$ columns of $\sqrt{N}\mathbf{F}_N$, and $\mathbf{D}_b = \text{diag}(\mathbf{B}\mathbf{b})$.

Define the channel estimate, estimation error and the MSE as $\hat{\mathbf{h}}$, $\mathbf{e} = \mathbf{h} - \hat{\mathbf{h}}$, and $\sigma^2 = \text{tr}\{\mathbb{E}[\mathbf{e}\mathbf{e}^{\mathcal{H}}]\}$, respectively, where $\mathbb{E}[.]$ is the expectation and tr(.) is the matrix trace. From [7], we know that the minimum MSE (MMSE) estimate, for white noise, is given by

$$\hat{\mathbf{h}} = \frac{1}{\mathcal{N}_0} \left(\mathbf{R}_h^{-1} + \frac{1}{\mathcal{N}_0} \mathbf{W}^{\mathcal{H}} \mathbf{W} \right)^{-1} \mathbf{W}^{\mathcal{H}} \hat{\mathbf{b}}, \quad (14)$$

where $\mathbf{R}_h = \mathbb{E}[\mathbf{h}\mathbf{h}^{\mathcal{H}}]$, $\mathcal{N}_0$ denotes the noise variance, and the matrix $\mathbf{W}$ depends on the scheme being used. When channel and noise statistics are not available at the receiver, least squares (LS) estimation can be used. The LS estimate is given by $\hat{\mathbf{h}} = (\mathbf{W}^{\mathcal{H}}\mathbf{W})^{-1}\mathbf{W}^{\mathcal{H}}\hat{\mathbf{b}}$.

The MSE of the estimate defined in Eq. (14) is given by

$$\sigma^2 = \text{tr}\left[\left(\mathbf{R}_h^{-1} + \frac{1}{\mathcal{N}_0} \mathbf{W}^{\mathcal{H}} \mathbf{W} \right)^{-1} \right] \geq \sum_{l=0}^{L} \frac{\sigma_{h_l}^2 \mathcal{N}_0}{\mathcal{N}_0 + \mathcal{P}_b \sigma_{h_l}^2}, \quad (15)$$

where $\mathcal{P}_b = \|\mathbf{b}\|^2$ is the pilot sub-block power, with $\|.\|$ being the L_2 norm, and $\sigma_{h_l}^2$, the channel tap variance. From Eq. (15), it can be seen that the lower bound is achieved when $\mathbf{R}_h$ and $\mathbf{W}^{\mathcal{H}}\mathbf{W}$ are diagonal. From Eq. (13), we know that $\mathbf{W} = \mathbf{D}_b \mathbf{T}_{\mathcal{I}_p} \mathbf{V}$, where $\mathbf{D}_b$ and $\mathbf{T}_{\mathcal{I}_p}$ are $N_p \times N_p$ and $N_p \times N$ matrices, respectively. Defining $\mathbf{V}_p = \mathbf{T}_{\mathcal{I}_p} \mathbf{V}$ as the rows of $\mathbf{V}$ indexed by $\mathcal{I}_p$, we observe that $\mathbf{W}^{\mathcal{H}}\mathbf{W} = \mathbf{V}_p^{\mathcal{H}} \mathbf{D}_b^{\mathcal{H}} \mathbf{D}_b \mathbf{V}_p$.

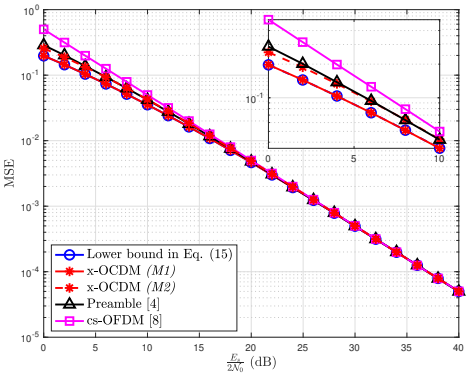

Fig. 1: Channel estimation MSE and the MSE lower bound in Eq. (15). Results for [4], [8] are only presented for *(M1)*.

If the pilots are equi-powered, $\mathbf{W}^{\mathcal{H}}\mathbf{W} = (\mathcal{P}_b/N_p)\mathbf{V}_p^{\mathcal{H}}\mathbf{V}_p$. If the pilots are equi-spaced and $N_p \geq L+1$, $\mathbf{V}_p^{\mathcal{H}}\mathbf{V}_p = N_p\mathbf{I}$. Note that this is possible for all of the considered schemes by defining $\mathcal{I}_p$ appropriately. Thus, $\mathbf{W}^{\mathcal{H}}\mathbf{W} = \mathcal{P}_b\mathbf{I}$ and the lower bound is achieved for each of the proposed schemes as long as channel taps are uncorrelated, i.e., $\mathbf{R}_h$ is diagonal. The following remark compares the spectral efficiency of the proposed estimators with existing ones in [4], [8].

Remark on spectral efficiency: For simplicity, let us assume that the channel remains static for two multicarrier blocks. In [4], a length$-P$ preamble is used to estimate the channel, where $P = N + N_{\text{CP}}$. At most, it can employ N symbols for data. Thus, the spectral efficiency is $\eta = N/2P$. In [8], a single pilot and $2L$ reserved subcarriers are used for channel estimation. Thus, its spectral efficiency is given by $\eta = (2N - 2L - 1)/2P$. We have already shown that the proposed methods require only $L+1$ pilots. Hence, spectral efficiency is given by $\eta = (2N - L - 1)/2P$. Since $L \ll N$ for most wireless channels, it is easy to see that the proposed methods offer better spectral efficiency. This is easily extended to channels that remain static for more than two block periods.

V. Analysis

We employ simulations to verify the performance of the proposed schemes and compare it to the schemed in [4], [8]. We fix $N = 1,024$ and $N_p = L + 1 = 64$ and employ 4-QAM and binary phase shift keying (BPSK) modulation, with the same average energy per symbol, for the data and pilots, respectively. We assume the channel is quasi-static with complex Gaussian channel taps and consider three variations of this model. *(M1)* Independent taps with an exponential power delay profile (PDP) given by $\sigma_{h_l}^2 = 0.9^l/\lambda,\ \forall l \in [0,\ L]$, where λ is a normalization constant such that $\sum_l \sigma_{h_l}^2 = 1$. *(M2)* Correlated taps with correlation matrix $\mathbf{R}_h$ given by $\mathbb{E}[h_n h_m^{\star}] = 1/(L+1),\ \forall m = n$; $\mathbb{E}[h_n h_m^{\star}] = \rho/(L+1),\ \forall m = n+1$; $\mathbb{E}[h_n h_m^{\star}] = \rho^2/(L+1),\ \forall m = n+2$; and 0 otherwise, where $\rho = 0.6$. *(M3)* Independent taps with uniform PDP, i.e., $\sigma_{h_l}^2 = 1/(L+1),\ \forall l$.

Fig. 1 compares the channel estimation performance of the proposed schemes (x-OCDM) and shows that the lower bound is indeed achieved when the channel taps are uncorrelated *(M1)*. The schemes in [4], [8] perform worse in low SNR and

This article has been accepted for publication in a future issue of this journal, but has not been fully edited. Content may change prior to final publication. Citation information: DOI 10.1109/LCOMM.2021.3124627, IEEE Communications Letters

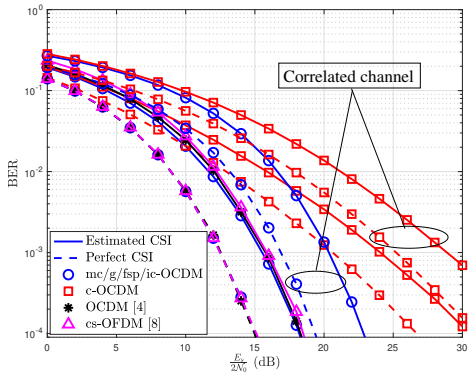

Fig. 2: BER comparison with perfect CSI and estimated CSI for channel *(M1)* and *(M2)*.

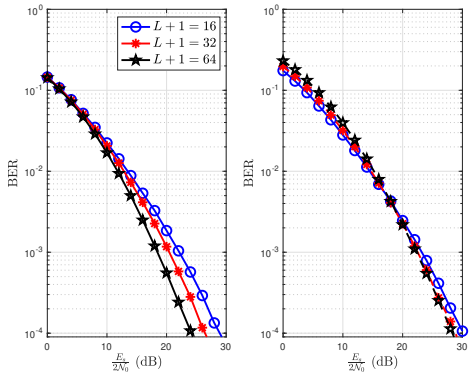

Fig. 3: BER comparison for c-OCDM with $N_p = 64$ and variable L with (left) ideal CSI and (right) estimated CSI for uniform PDP *(M3)*.

similar to x-OCDM at high SNR. Tap correlation *(M2)* leads to higher MSE at lower SNR, but as the MSE increases, the contribution of $\mathbf{R}_h$ in Eq. (15) decreases and thus, the MSE converges to the lower bound.

The average BER of the considered schemes for *(M1)* are presented in Fig. 2. Results show that all of the proposed schemes show the same performance as OCDM with channel estimation errors accounting for the 3 dB gap between the estimated and perfect CSI cases. However, c-OCDM performs the worst of all the considered schemes due to frequency-localized spreading of the data. This occurs because adjacent frequencies experience correlated fading when $N > L + 1$. Thus, a deep fade may affect an entire sub-band, limiting the average performance. This is not the case for the other proposed schemes as data is spread over uncorrelated frequencies which mitigates deep fades. Channel correlations *(M2)* affect the proposed schemes similarly. Fig. 2 shows that c-OCDM and mc-OCDM suffer from similar deterioration as more subcarriers are likely to experience deep fades, creating a performance bottleneck.

Fig. 3 shows that c-OCDM transmissions show better performance with ideal CSI as the channel delay spread increases, while the sub-block size is kept constant, i.e., $J = 15$. Typically, $N \gg L$, and thus, c-OCDM spreads data over a subset of neighboring, correlated subcarriers. Smaller L corresponds to stronger correlations among neighboring subcarriers so deep fades have a greater impact on the sub-block detection performance. The difference in performance is apparent for high SNR as noise becomes negligible. On the other hand, when perfect CSI is not available, Fig. 3 shows similar performance. This occurs because larger L increases the MSE of channel estimation, which can be inferred from Eq. (15). Thus, larger channel estimation errors counteract the performance gains seen due to larger delay spreads.

Thus far, results show that channel estimation performance is exactly the same for the proposed schemes. However, we have already seen that c-OCDM suffers performance deterioration in terms of BER due to constrained spreading. Furthermore, the sub-block sizes are restricted in the interleaved schemes, i.e., ic/g/fsp-OCDM. Let K denote the sub-block size and N, the block size. By construction it follows that $N/K \in \mathbb{Z}^+$, where $\mathbb{Z}^+$ is the set of positive integers, and that $N/K > 1$. Now, recall that $K \geq L+1$ for channel estimation with maximum spectral efficiency when $K = L+1$. However, it is not necessary that $N/(L+1)$ is an integer, in which case $K > L + 1$. This leads to some loss in spectral efficiency. Thus, for these reasons mc-OCDM has a distinct advantage since it shows the best BER performance and allows for the greatest flexibility in terms of the pilot sub-block size.

VI. Conclusions

In this letter, we proposed various schemes to enable pilot-based channel estimation for OCDM. The proposed schemes show the same performance in terms of estimation quality and can achieve the MSE lower bound for uncorrelated channel taps despite having higher spectral efficiency than other proposed methods. Moreover, all schemes, except c-OCDM, show the same BER as conventional OCDM. In the future, we will extend this work to doubly-selective channels.

References

[1] X. Ouyang and J. Zhao, "Orthogonal chirp division multiplexing," *IEEE Trans. Commun.*, vol. 64, no. 9, pp. 3946–3957, 2016.

[2] M. S. Omar and X. Ma, "Performance analysis of OCDM for wireless communications," *IEEE Trans. Wireless Commun.*, pp. 1–1, 2021.

[3] R. Bomfin, D. Zhang, M. Matthé, and G. Fettweis, "A theoretical framework for optimizing multicarrier systems under time and/or frequency-selective channels," *IEEE Commun. Lett.*, vol. 22, no. 11, pp. 2394–2397, 2018.

[4] X. Ouyang, C. Antony, G. Talli, and P. D. Townsend, "Robust channel estimation for coherent optical orthogonal chirp-division multiplexing with pulse compression and noise rejection," *J. Lightw. Technol.*, vol. 36, no. 23, pp. 5600–5610, 2018.

[5] R. Bomfin, M. Chafii, A. Nimr, and G. Fettweis, "A robust baseband transceiver design for doubly-dispersive channels," *IEEE Trans. Wireless Commun.*, pp. 1–1, 2021.

[6] S. Ohno and G. B. Giannakis, "Optimal training and redundant precoding for block transmissions with application to wireless OFDM," *IEEE Trans. Commun.*, vol. 50, no. 12, pp. 2113–2123, 2002.

[7] ——, "Capacity maximizing MMSE-optimal pilots for wireless OFDM over frequency-selective block Rayleigh-fading channels," *IEEE Trans. on Inf. Theory*, vol. 50, no. 9, pp. 2138–2145, 2004.

[8] K. Ozaki, K. Tomitsuka, A. Okazaki, H. Sano, and H. Kubo, "Channel estimation technique for OFDM systems spread by chirp sequences," in *Proc. IEEE 23rd Int. Symp. Pers., Indoor Mobile Radio Commun. (PIMRC)*, 2012.

[9] M. S. Omar and X. Ma, "Designing OCDM-based multi-user transmissions," in *Proc. 2019 IEEE Global Commun. Conf. (GLOBECOM)*, 2019.

[10] ——, "Spectrum design for orthogonal chirp division multiplexing transmissions," *IEEE Wireless Commun. Lett.*, vol. 9, no. 11, pp. 1990–1994, 2020.